Multi-step structural phase transitions with novel symmetry breaking and inverse symmetry breaking characteristics in a $[Ag_4I_6]^{2-}$ cluster hybrid crystal

Jin Zhang,[a] Wan-Wan Yao,[a] Lei Sang,[a] Xue-Wei Pan,[a] Xiao-Zu Wang,* [b] Wen-Long Liu,[c] Lifeng Wang,[d] Xiao-Ming Ren* [a, e]

[a] State Key Laboratory of Materials-Oriented Chemical Engineering and College of Chemistry and Molecular Engineering, Nanjing Tech University, Nanjing 211816, P. R. China

[b] College of Chemical Engineering, Nanjing Tech University, Nanjing 211816, P. R. China

[c] College of Chemistry and Chemical Engineering, Yangzhou University, Yangzhou 225002, P. R. China

[d] Institute for Frontier Materials (IFM), Deakin University, 75 Pigdons Road, Waurn Ponds, Victoria 3216, Australia

[e] State Key Laboratory of Coordination Chemistry, Nanjing University 210023, P. R. China

Tel: 86-25-58139476

E-mail: xmren@njtech.edu.cn

Experimental section

All reagents and materials were purchased from commercial sources and directly used without further purification.

Synthesis of 1-Propyl-1, 4-diazabicyclo[2.2.2]octan-1-ium bromide

1-Propyl-1,4-diazabicyclo[2.2.2]octan-1-ium bromide ([Pr-dabco]Br) was synthesized using a modified procedure reported previously.[1] Dabco (1.12 g, 10 mmol) was dissolved in acetone (50 mL) and 1-bromopropane (1.23 g, 10 mmol) was added dropwise into the dabco acetone solution under magnetic stirring. The colorless oily precipitate formed two hours later, which was collected by centrifuge, washed with ethyl acetate for three times (5 mL per time), and dried under vacuum at ambient temperature. The yield is ~84%. [Pr-dabco]Br was characterized by ^{1}H NMR (ref. Figure S1).

Synthesis of $C_{18}H_{38}N_4Ag_4I_6$ (1)

AgI (0.235 g, 1 mmol) was added into KI saturated solution in mixed water (5 mL) with acetonitrile (12 mL), and then [Pr-dabco]Br (0.353g , 1.5 mmol) in CH_3OH 4 mL was added dropwise to the above mixture. The colorless polyhedral-shaped crystals formed when the mixture was standed 5 day later at ambient temperature, which were separated by filtration, washed with ethanol for three times (~5 mL per time) and finally dried at ambient temperature. The yield of crystalline sample is ~48% calculated on the basis of the reactant of AgI amount. Elemental analysis calculated for $C_{18}H_{38}N_4Ag_4I_6$ (%): C 14.36, H 2.53, N 3.72. Found: C 14.38, H 2.63, N 3.64. IR spectroscopy (KBr pellet, cm^{-1}; Figure S2): 2972s,$\nu_{as}(CH_3)$, 2928s,$\nu_{as}(CH_2)$, 2882s,$\nu_s(CH_3)$, 1458s,$\delta_s(CH_2)$ and $\delta_{as}(CH_3)$, 1373s, $\delta_s(CH_3)$, 1321s, ν(C-N), 1092s, ν(C-N), 1054s, ν(C-N), 1004s, ν(C-N),840s $\delta(CH_2)_2$, 795s $\delta(CH_2)_2$.

Chemical Analysis and Physical Measurements

Elemental analyses for C, H and N were performed with an Elementar Vario EL III analytic instrument. Fourier transform infrared (FTIR) spectrum was collected on a Nicolet iS5 spectrometer with KBr pellets in the spectral regime of 400-4000 cm^{-1}. ^{1}H-NMR spectroscopy was run at 400 MHz in DMSO-d6 on Bruker-DPX-200 instruments. UV-visible absorbance was collected in the solid state at room temperature on a Perkin–Elmer Lambda 950 UV-vis spectrometer equipped with Labsphere integrating over the spectral range 200–800 nm using KBr pellet as

reflectance standards (Figure S3). Powder X-ray diffraction (PXRD) data were recorded on a Bruker D8 Discover diffractometer with Cu Kα radiation (λ = 1.54056 Å) with a scan speed of 5°/min and a step size of 0.02° in 2θ at room temperature. The variable-temperature PXRD measurements were performed using a Shimadzu XRD-6100 diffractometer operating with a Cu Kα radiation source (λ = 1.5418 Å) in the temperature range of 303~473K. During the measurements of the temperature-dependent PXRD data, the temperature changing rate is 10 K min^{-1}. It is worth mentioning that the PXRD measurement at a certain temperature starts after the sample is kept at the set temperature for 15 minutes to ensure that the sample and probe have the same temperature.

Thermal gravimetric analyses (TGA) were performed using a DTA-TGA 2960 thermogravimetric analyzer in nitrogen atmosphere with a heating rate of 10 K/min in 293-873 K (20~600 °C). Differential scanning calorimetry (DSC) measurements were carried out on a NETZSCH DSC 204F1 Phoenix calorimeter for powdered samples in 253-453 K (-20~180 °C) with a temperature scanning rate of 10 °C/min.

The measurements of dielectric, impedance spectra and ac conductivities were performed for the powdered sample, which is prepared into a disk form with a diameter of 7 mm and a thickness of 0.95 mm and sandwiched between two parallel platinum electrodes, using a Concept 80 system (Novocontrol, Germany), the measurement was performed under N_2 atmosphere in the temperature range of 253-453 K and the frequency range of 1-10^7 Hz.

X-ray crystallography

Single crystal X-ray diffraction data were collected on a Bruker SMART CCD area detector at 293, 323 and 408 K, respectively, using the graphite-monochromated Mo K_α (λ = 0.71073 Å) radiation. Data reductions and absorption corrections were performed with the SAINT[2] and SADABS2[3] software packages, respectively. Structures were solved by direct method using the SHELXL–2014[4] software package. The non-hydrogen atoms were anisotropically refined using the full matrix least-squares method on F^2. All the hydrogen atoms were geometrically fixed and placed in ideal positions in the structures at 293 and 323 K. The alkyl chain in Pr-dabco$^+$ and $[Ag_4I_6]^{2-}$ cluster show disorder in the crystal structure at 408 K, thus, both alkyl chain and $[Ag_4I_6]^{2-}$ cluster are refined using three parts disorder model. The details about data collection, structural refinement and crystallography are listed in Table S1.

References

1. J.-Y. Kazock, M. Taggougui, B. Carré, P. Willmann, D. Lemordanta, Synthesis, 2007, 24, 3776−3778.
2. Bruker, APEX 2, SAINT, XPREP, Bruker AXS Inc., Madison, Wisconsin, USA, 2007.
3. Bruker, SADABS, Bruker AXS Inc., Madison, Wisconsin, USA, 2001.
4. G. M. Sheldrick, SHELXS–2014, Program for the solution and refinement of crystal structures, University of Göttingen, Göttingen, Germany, 2014.

Table S1: Crystallographic data and refinement parameter of **1** at 293, 323 and 408 K

Temp. / K	293	323	408
CCDC no.	1961530	1961531	1961690
Empirical formula	$C_{18}H_{38}Ag_4I_6N_4$	$C_{18}H_{38}Ag_4I_6N_4$	$C_{18}H_{38}Ag_4I_6N_4$
Formula weight	1503.40	1503.40	1503.40
Crystal system	Orthorhombic	Monoclinic	Cubic
Space group	*Pbca*	$P2_1/c$	*Pa-3*
a/Å	14.9129(5)	15.0205(8)	15.1410(9)
b/Å	14.9759(6)	15.0458(10)	15.1410(9)
c/Å	15.1499(5)	15.0407(10)	15.1410(9)
α/°	90	90	90
β/°	90	90.269(2)	90
γ/°	90	90	90
V/Å^3 / Z	3383.5/2	3399.1/4	3471.1/4
Calc. density g/cm	2.951	2.938	2.877
Abs. coeff. μ/mm^{-1}	7.771	7.735	7.575
F(000)	2720	2720	2720
θ range for data collection/°	2.35 to 27.285	2.712 to 50	5.38 to 55.226
Index ranges	$-19 \le h \le 19$ $-15 \le k \le 19$ $-16 \le l \le 19$	$-17 \le h \le 16$ $-15 \le k \le 17$ $-12 \le l \le 17$	$-19 \le h \le 16$ $-19 \le k \le 12$ $-19 \le l \le 16$
Refl. collected/ unique	35814 / 3907	28919/5862	33119/1356
R(int)	0.0381	0.0596	0.0740
Goodness-of-fit on F^2	1.066	1.010	1.074
Final R indices [I>2sigma(I)]	R1 = 0.0482 wR2 = 0.1108	R_1= 0.1746 wR_2= 0.2956	R_1= 0.0584 wR_2= 0.1281
R indices (all data)	R1 = 0.0640 wR2 = 0.1182	R_1= 0.1774 wR_2= 0.2958	R_1= 0.1170 wR_2= 0.1479
Residual (e Å^{-3})	3.3 /-1.98	1.57/-1.04	0.54/-0.50

[a] $R_1 = \sum||F_o| - |F_c|/\sum|F_o|$; $wR_2 = \{\sum[w(F_o^2 - F_c^2)^2]/\sum[w(F_o^2)^2]\}^{1/2}$

Table S2: Bond lengths (Å) in $[Ag_4I_6]^{2-}$ cluster at 293, 323 and 408 K

T = 293 K		T = 323 K		T = 408 K	
Atom pair	distance	Atom pair	distance	Atom pair	distance
I1-Ag1	2.8230(10)	I1-Ag1	2.878(10)	I1-Ag2$^{\#3}$	2.836(15)
I1-Ag2	2.7753(10)	I1-Ag2	2.820(10)	I1-Ag2	2.745(10)
I3-Ag1$^{\#1}$	2.8427(10)	I3-Ag1$^{\#1}$	2.840(10)	I1-Ag1$^{\#1}$	2.723(13)
I3-Ag2	2.7645(11)	I3-Ag2	2.779(10)	I1-Ag1	3.105(19)
I2-Ag1	2.8796(11)	I2-Ag1	2.861(10)	I1-Ag1$^{\#2}$	3.12(3)
I2-Ag2	3.1344(14)	I2-Ag2	3.076(10)	Ag1-Ag2$^{\#3}$	3.037(12)
I2-Ag2$^{\#1}$	3.0652(14)	I2-Ag2$^{\#1}$	3.058(11)	Ag1-Ag2$^{\#5}$	2.938(5)
Ag1-Ag2	2.9846(11)	I4-Ag3	2.844(11)	Ag2-Ag1$^{\#5}$	2.938(5)
Ag1-Ag2$^{\#1}$	3.0320(11)	I4-Ag4	2.757(11)	Ag2-Ag1$^{\#}$	2.865(10)
Ag2-Ag2$^{\#1}$	2.9326(18)	I6-Ag3$^{\#2}$	2.821(10)	N1-Ag1	2.451(11)
Ag1-N1	2.421(7)	I6-Ag4	2.796(11)	N1-Ag1$^{\#1}$	2.451(11)
		I5-Ag3	2.910(11)	N1-Ag1$^{\#2}$	2.454(11)
		I5-Ag4	3.262(14)		
		I5-Ag4$^{\#2}$	3.182(14)		
		Ag1-Ag2	3.034(11)		
		Ag1-Ag2$^{\#1}$	2.978(10)		
		Ag3-Ag4$^{\#2}$	2.969(11)		
		Ag3-Ag4	3.037(12)		
		Ag2-Ag2$^{\#1}$	2.944(16)		
		Ag4-Ag4$^{\#2}$	2.856(18)		
		Ag1-N1	2.49(2)		
		Ag3-N3	2.50(2)		

Symmetry codes:

T = 293 K

#1 = 1 - x, 1 - y, 1 - z

T = 323 K

#1 = 1 - x, 2 - y, 1 - z

#2 = -x, 1 - y, 1 - z

T = 408 K

#1 = 3/2 - y,1 -z, -1/2 + x

#2 = 1/2 + z, 3/2 - x, 1- y

#3 = 1/2 + y, + z, 3/2 - x

#4 = 3/2 - z, -1/2 + x, + y

#5 = 2 - x, 1 - y, 1 - z

Table S3: Bond lengths (Å) in Pr-dabco^{+} moiety at 293, 323 and 408 K

T = 293 K		T = 323 K		T = 408 K	
Atom pair	distance	Atom pair	distance	Atom pair	distance
N2-C6	1.507(10)	N1-C1	1.500(9)	C1-N1	1.458(9)
N2-C7	1.507(10)	N1-C3	1.493(9)	C1-C2	1.509(12)
N2-C4	1.504(10)	N1-C5	1.497(9)	N2-C2	1.502(9)
N2-C2	1.505(10)	N2-C2	1.497(9)	N2-C3	1.47(2)
N1-C5	1.460(11)	N2-C4	1.500(9)	C3-C4	1.431(18)
N1-C3	1.496(11)	N2-C6	1.496(9)	C5-C4	1.564(18)
N1-C1	1.479(11)	N2-C13	1.505(10)		
C6-C5	1.546(12)	C1-C2	1.523(9)		
C7-C8	1.491(13)	C3-C4	1.521(9)		
C8-C9	1.519(13)	C5-C6	1.522(9)		
C4-C3	1.530(12)	C13-C14	1.554(10)		
C2-C1	1.519(12)	C14-C15	1.558(10)		
		N3-C7	1.493(9)		
		N3-C9	1.498(9)		
		N3-C11	1.498(9)		
		N4-C8	1.499(9)		
		N4-C10	1.496(9)		
		N4-C12	1.496(9)		
		N4-C16	1.506(10)		
		C7-C8	1.521(9)		
		C9-C10	1.522(9)		
		C11-C12	1.521(9)		
		C16-C17	1.545(10)		
		C17-C18	1.552(10)		

Symmetry codes:

T = 293 K

#1 = 1 - x, 1 - y, 1 - z

T = 323 K

#1 = 1 - x, 2 - y, 1 - z

#2 = -x, 1 - y, 1 - z

T = 408 K

#1 = 3/2 - y,1 -z, -1/2 + x

#2 = 1/2 + z, 3/2 - x, 1- y

#3 = 1/2 + y, + z, 3/2 - x

#4 = 3/2 - z, -1/2 + x, + y

#5 = 2 - x, 1 - y, 1 - z

Table S4: Bond angles (°) in $[Ag_4I_6]^{2-}$ cluster at 293, 323 and 408 K

T = 293 K		T = 323 K		T = 408 K	
Atoms	Angle	Atoms	Angle	Atoms	Angle
I1-Ag1-I3$^{\#1}$	132.43(4)	N1-Ag1-I1	105.7(9)	N1-Ag1-I1$^{\#2}$	106.5(5)
I1-Ag1-I2	105.59(3)	N1-Ag1-I3$^{\#1}$	99.1(10)	Ag1$^{\#1}$-I1-Ag2$^{\#3}$	63.8(3)
I3$^{\#1}$-Ag1-I2	105.52(3)	N1-Ag1-I2	106.2(9)	Ag1$^{\#1}$-I1-Ag2	63.2(2)
N1-Ag1-I1	105.84(16)	N3-Ag3-I4	103.0(11)	Ag2-I1-Ag1$^{\#2}$	60.90(19)
N1-Ag1-I3$^{\#1}$	98.23(16)	N3-Ag3-I6$^{\#2}$	100.6(11)	Ag2-I1-Ag1	63.3(2)
N1-Ag1-I2	107.14(17)	N3-Ag3-I5	106.9(11)	Ag2$^{\#3}$-I1-Ag1$^{\#2}$	63.8(2)
I1-Ag2-I2	100.28(3)	I1-Ag2-I2	100.5(3)	Ag2$^{\#3}$-I1-Ag1	61.3(2)
I1-Ag2-I2$^{\#1}$	103.84(4)	I1-Ag2-I2$^{\#1}$	101.9(3)		
I3-Ag2-I1	131.79(4)	I1-Ag1-I3$^{\#1}$	131.3(3)		
I3-Ag2-I2$^{\#1}$	102.66(3)	I1-Ag1-I2	104.4(3)		
I3-Ag2-I2	97.53(4)	I2-Ag2-I2$^{\#1}$	122.6(3)		
I2$^{\#1}$-Ag2-I2	123.55(3)	I3-Ag2-I1	132.1(3)		
		I3-Ag2-I2	98.1(3)		
		I3-Ag2-I2$^{\#1}$	104.3(3)		
		I3^{1}-Ag1-I2	107.9(3)		
		I4-Ag3-I5	105.3(3)		
		I4-Ag4-I6	131.2(4)		
		I4-Ag4-I5	98.6(3)		
		I4-Ag4-I5$^{\#2}$	102.6(4)		
		I5$^{\#2}$-Ag4-I5	127.4(3)		
		I6-Ag4-I5$^{\#2}$	102.1(3)		
		I6-Ag4-I5	98.8(4)		
		I6$^{\#2}$-Ag3-I4	130.3(4)		
		I6$^{\#2}$-Ag3-I5	108.6(3)		

Symmetry codes:

T = 293 K

#1 = 1 - x, 1 - y, 1 - z

T = 323 K

#1 = 1 - x, 2 - y, 1 - z

#2 = -x, 1 - y, 1 - z

T = 408 K

#1 = 3/2 - y,1 -z, -1/2 + x

#2 = 1/2 + z, 3/2 - x, 1- y

#3 = 1/2 + y, + z, 3/2 - x

#4 = 3/2 - z, -1/2 + x, + y

#5 = 2 - x, 1 - y, 1 - z

(a)

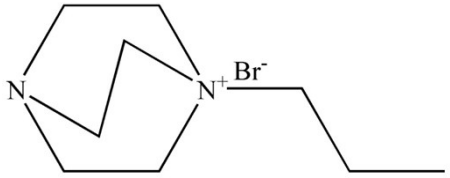

1-Propyl-1,4-diazabicyclo[2.2.2]octan-1-ium bromide

(b)

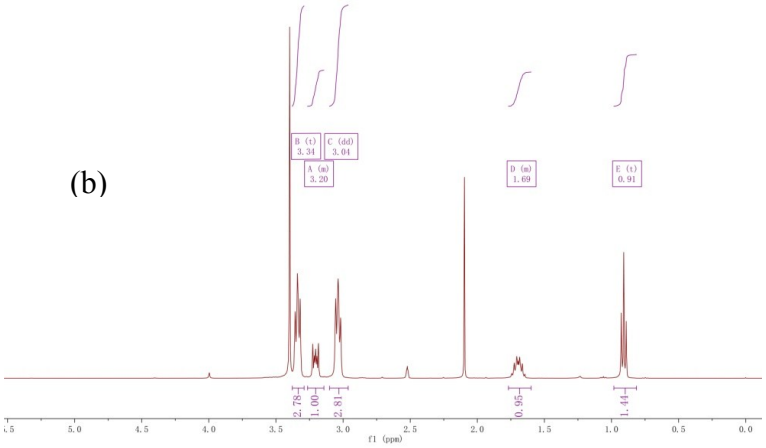

Figure S1: (a) Scheme of molecule structure of [Pr-dabco]Br and (b) its ^{1}H-NMR spectrum ^{1}H NMR (400 MHz, DMSO-d_6): d = 3.34 (6 H, 3 CH_2), 3.20 (2 H, CH_2), 3.04 (6 H, 3 CH_2), 1.69 (2 H, CH_2), 0.91 (3 H, CH_3), 2.5 (DMSO-d_6), 4.0 (ethyl acetate), 2.1 (ethyl acetate).

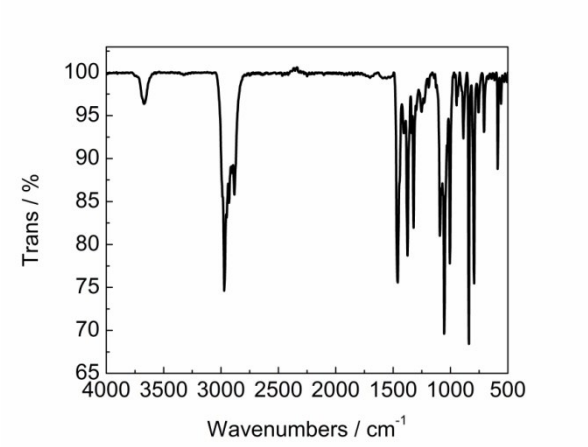

Figure S2: IR spectrum of $(Pr\text{-}dabco)_2Ag_4I_6$.

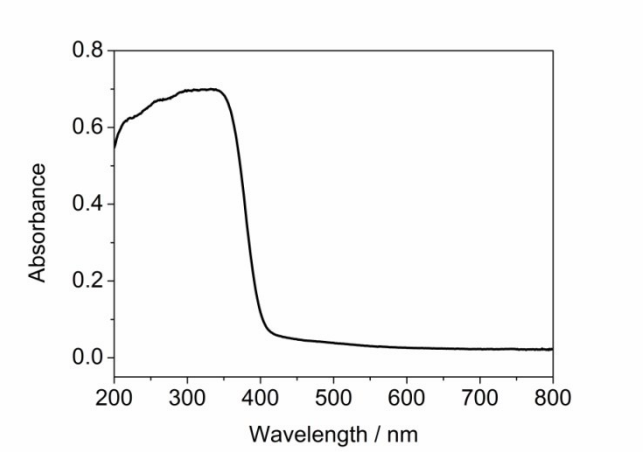

Figure S3: Diffuse reflection spectrum of $(Pr\text{-}dabco)_2Ag_4I_6$.

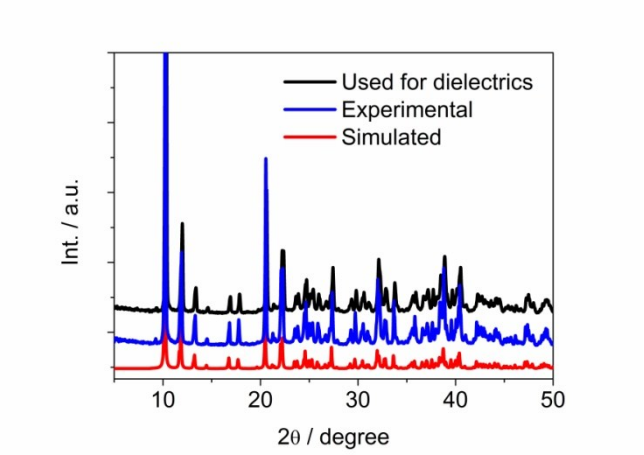

Figure S4: Room temperature (293 K) PXRD patterns of the samples after dielectric measurement for three thermal cycles in 253-453 K, the soaked in water for one month and the simulated PXRD pattern of $(Pr\text{-}dabco)_2Ag_4I_6$ in phase-I.

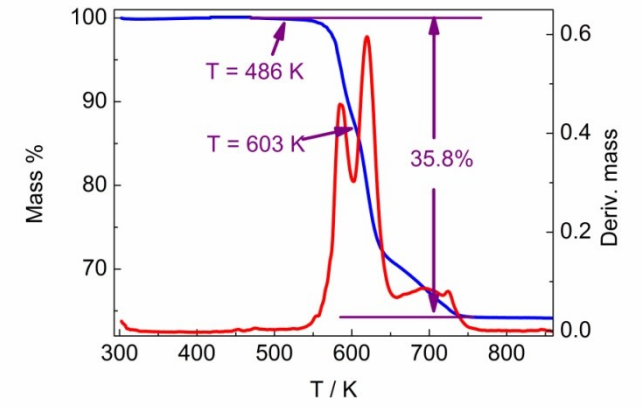

Figure S5: TG and its derivative plot of $(Pr\text{-}dabco)_2Ag_4I_6$.

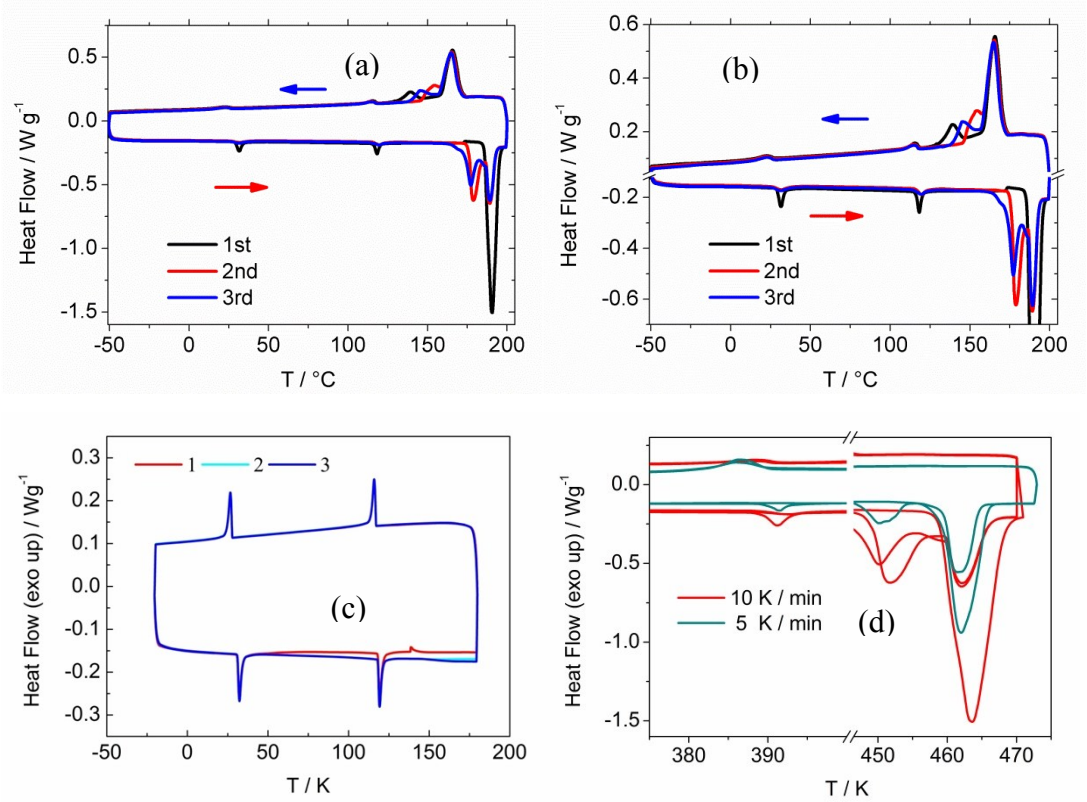

Figure S6: DSC plots of $(Pr\text{-}dabco)_2Ag_4I_6$ performed three successive thermal cycles (a, b) between -50 and 200 °C (223-473 K) and (c) between -20 and 180 °C (253-453 K) with temperature scanning rate of 10 K/min; (d) comparison of DSC plots at different temperature scanning rates, indicating that there is no significant distinction between temperature scanning rates of 5 and 10 K /min.

(a)

(b)

Figure S7: The morphologies of crystals of (Pr-dabco)2Ag4I6 at (a) room temperature and (b) heated at 473 K for one hour.

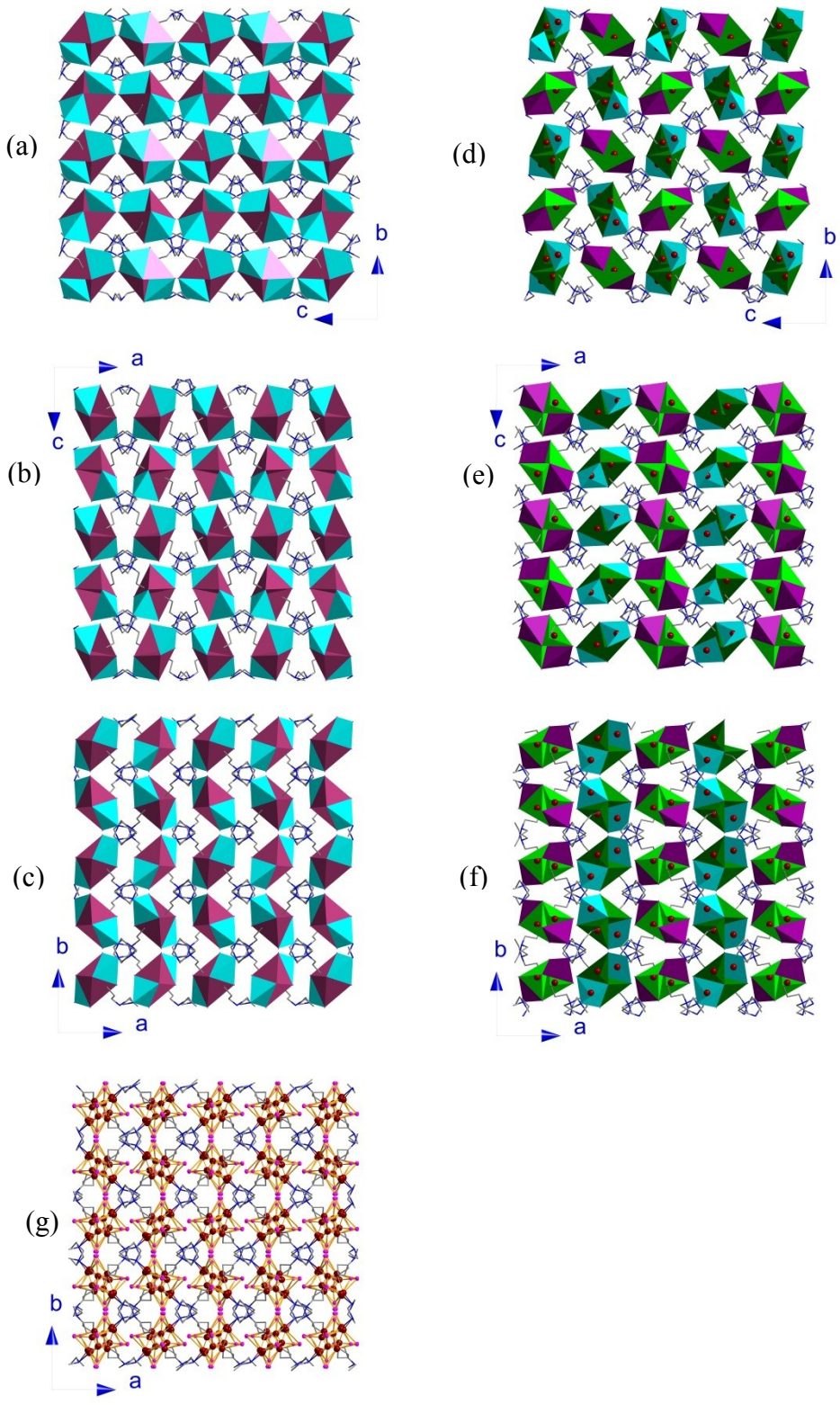

Figure S8: Packing diagrams of (Pr-dabco)$_2$Ag$_4$I$_6$ viewed along (a-c) *a*-, *b*- and *c*-axes in phase-I (d-f) *a*-, *b*- and *c*-axes in phase-I I (g) *c*-axis in phase-III. In (a-f), different color tetrahedra represent different Ag tetrahedra, respectively.

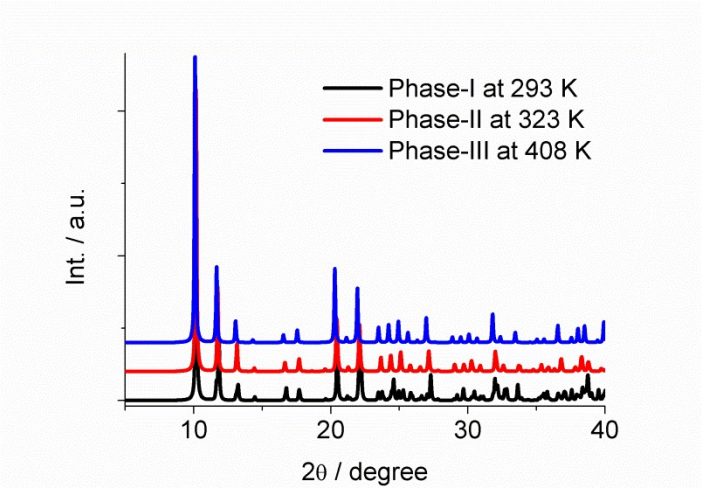

Figure 9: The simulated PXRD patterns of $(Pr\text{-}dabco)_2Ag_4I_6$ in phase-I at 293 K, phase-II at 323 K and 408 K, respectively.

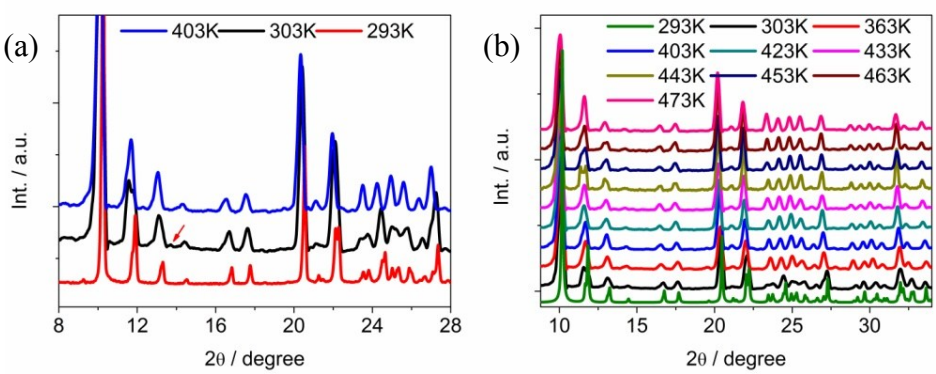

Figure 10: Variable-temperature PXRD patterns for the polycrystalline sample of $(Pr\text{-}dabco)_2Ag_4I_6$ at the (a) selected temperatures and (b) cooling runs.

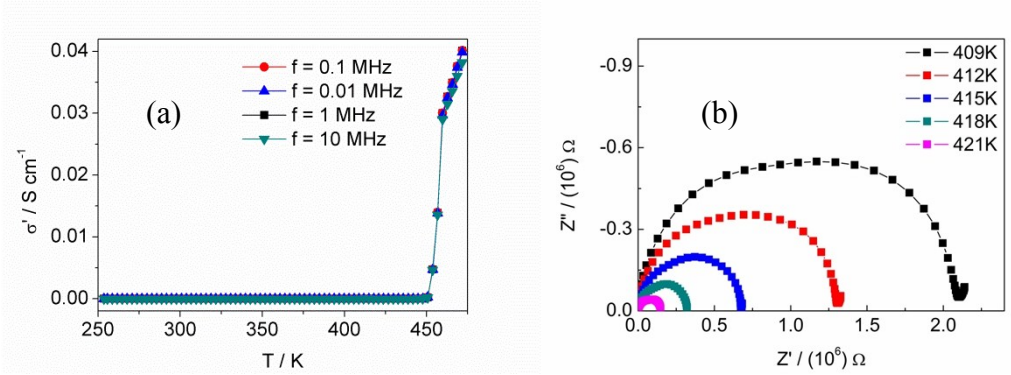

Figure S11: (a) Variable temperature ac conductivity at the selected frequencies (b) Nyquist plots in the temperature range of 436-448 K for $(Pr\text{-}dabco)_2Ag_4I_6$.